A novel arylpiperazine derivative (LQFM181) protects against neurotoxicity induced by 3- nitropropionic acid in in vitro and in vivo models

A novel arylpiperazine derivative (LQFM181) protects against neurotoxicity induced by 3-nitropropionic acid in *in vitro* and *in vivo* models

Hericles Mesquita Campos[a], Robbert Mota Pereira[a], Pâmela Yasmin de Oliveira Ferreira[a], Nkaa Uchenna[a], Cínthia Rio Branco da Silva[a], Letizia Pruccoli[b], Germán Sanz[c], Marcella Ferreira Rodrigues[c], Boniek Gontijo Vaz[c], Bárbara Gonçalves Rivello[d], André Luís Batista da Rocha[d], Flávio Silva de Carvalho[d], Gerlon de Almeida Ribeiro Oliveira[e], Luciano Morais Lião[c], Raphaela de Castro Georg[a], Jacqueline Alves Leite[a], Fernanda Cristina Alcantara dos Santos[a], Elson Alves Costa[a], Ricardo Menegatti[d], Andrea Tarozzi[b], Paulo César Ghedini[a *]

[a] Institute of Biological Sciences, Federal University of Goias, Goiania, GO, Brazil

[b] Department of Life Quality Studies, Alma Mater Studiorum - University of Bologna, Rimini, Italy

[c] Chemistry Institute, Federal University of Goias, Goiania, GO, Brazil

[d] Faculty of Pharmacy, Laboratory of Medicinal Pharmaceutical Chemistry, Federal University of Goias, Goiania, GO, Brazil

[e] Department of Pharmacy, Faculty of Health Sciences, University of Brasilia, Brasilia, DF, Brazil

* Corresponding author: Biochemical and Molecular Pharmacology Laboratory, Institute of Biological Sciences, Federal University of Goias, Cep 74690-900, Goiania, GO, Brazil.

E-mail: pcghedini@ufg.br; phone +55 62 3521-1725

Abstract

In the pursuit of novel antioxidant therapies for the prevention and treatment of neurodegenerative diseases, three new arylpiperazine derivatives (LQFM181, LQFM276, and LQFM277) were synthesized through a molecular hybridization approach involving piribedil and butylated hydroxytoluene lead compounds. To evaluate the antioxidant and neuroprotective activities of the arylpiperazine derivatives, we employed an integrated approach using both *in vitro* (SH-SY5Y cells) and *in vivo* (neurotoxicity induced by 3-nitropropionic acid in Swiss mice) models. In the *in vitro* tests, LQFM181 showed the most promising antioxidant activity at the neuronal membrane and cytoplasmic levels, and significant neuroprotective activity against the neurotoxicity induced by 3-nitropropionic acid. Hence, this compound was further subjected to *in vivo* evaluation, which demonstrated remarkable antioxidant capacity such as reduction of MDA and carbonyl protein levels, increased activities of succinate dehydrogenase, catalase, and superoxide dismutase. Interestingly, using the same *in vivo* model, LQFM181 also reduced locomotor behavior and memory dysfunction through its ability to decrease cholinesterase activity. Consequently, LQFM181 emerges as a promising candidate for further investigation into its neuroprotective potential, positioning it as a new therapeutic agent for neuroprotection.

Key words: Arylpiperazine derivatives; Neuroprotection; Antioxidant activity; Anticholinesterase effect

1. Introduction

Neurodegenerative diseases (NDs) present a formidable challenge in contemporary neuroscience, encompassing critical areas such as current medical practices, medicinal chemistry, and the quest for novel therapeutic interventions [1]. These debilitating conditions, including Alzheimer's disease (AD), Parkinson's disease (PD), multiple sclerosis (MS) and Huntington's disease (HD), exert profound impacts on patients. The current therapeutic approaches for the management of NDs, including cholinesterase inhibitors and glutamate regulators for AD and dopamine supplements for PD, only control the progression of the disease rather than eliminate the root causes [2]. In an effort to combat NDs, the pursuit of groundbreaking treatments remains a top priority [3], encompassing advancements such as gene therapy [4] and treatments specifically targeting microglia [5].

Numerous signaling pathways have been unveiled within the intricate pathogenesis of NDs, notably those entwined with neuroinflammation, apoptosis, and oxidative stress (OS) [6]. The OS has a pivotal factor in the pathogenesis of NDs [7,8] where the dysregulation of reactive oxygen species (ROS), such as superoxide radicals ($O_2^{-\bullet}$), hydrogen peroxide (H_2O_2), and hydroxyl radicals ($OH^{-\bullet}$), contributes to lipid peroxidation (LPO), protein and DNA oxidation [9-11]. The elevated concentrations of ROS in brain tissues affect synaptic and non-synaptic communication between neurons and glia, resulting in neuroinflammation and neuronal death, which lead to neurodegeneration [12]. Hence, the investigation into antioxidant therapies has emerged as a compelling strategy for the prevention and treatment of NDs [13,14].

In light of this understanding, polyphenols emerge as promising candidates among these potential therapeutic avenues, given to their broad spectrum of neuroprotective attributes [12,15,16]. These include the capacity to mitigate OS and neuroinflammation, shield neurons from damage, and enhance cognitive functions such as mental acuity and memory. As highlighted by Islam et al. (2022) [12], the multifaceted capabilities of polyphenols position them as new potential strategy for the treatment and management of NDs. Additionally, another emerging therapeutic perspective lies in

marine carotenoids, which act on various pathological pathways, such as preventing the formation of free radicals and inhibiting the auto-oxidation chain reaction [17,18]. Bahbah et al. (2021) [6], described the potential neurotherapeutic effects of astaxantin, a marine carotenoid, which has been shown to mitigate neuroinflammation implicated in the pathology and progression of AD, PD, nerve injury, cerebral ischemia, and autism.

Among the array of compounds already under investigation for the treatment of brain diseases, arylpiperazine derivatives emerge as yet another potential agent. This class of compounds represents a chemical group with multifunctional neuroprotective activities, encompassing anti-inflammatory and antioxidative effects [19-24]. Moreover, they have been associated with cognitive enhancement in patients suffering from neurodegenerative conditions [25,26].

Notably, piribedil (**1**), an early member of piperazine class, was among the pioneering compounds marketed for NDs treatment, specifically targeting motor system dysfunction [27-29]. Experimental evidence further supports piribedil's efficacy, showing improvements in neurological function, memory, and learning in a rat model of cerebral ischemia and reperfusion, along with alleviation of motor symptoms in early and advanced stages of Parkinson's disease [30,31].

Moreover, previous studies have demonstrated the antioxidative potential of piperazine based compounds [22-24]. Notably, recent research unveiled LQFM212, a compound containing a piperazine ring and synthesized through molecular hybridization between LQFM032, with anxiolytic-like activity, and butylated hydroxytoluene (BHT) (**2**), a gold standard antioxidant. LQFM212 showed the ability to mitigate neuroinflammation-induced behavioral, inflammatory, and oxidative changes through its antioxidant properties [32].

Given these compelling observations and the capacity of arylpiperazine derivatives to modulate their pharmacological profiles through structural variations, coupled with their synergistic antioxidative effects [33], the present study aimed to synthesize three novel arylpiperazine derivatives through the molecular hybridization strategy using piribedil (**1**) and BHT (**2**) lead compounds: 2,6-di-*tert*-butyl-4-((4-phenylpiperazin-1-yl)methyl)phenol (LQFM181) (**3**), 2,6-di-*tert*-butyl-4-((4-(4-

hydroxyphenyl)piperazin-1-yl)methyl)phenol (LQFM276) (**4**), and 2,6-di-*tert*-butyl-4-((4-(4-methoxyphenyl)piperazin-1-yl)methyl)phenol (LQFM277) (**5**) (Fig. 1). We assessed the antioxidant and neuroprotective effects of the arylpiperazine derivatives using a combined experimental approach of *in vitro* and *in vivo* models. We initially evaluated the *in silico* ADME, neurotoxicity and antioxidant activity of the new arylpiperazine derivatives in neuronal SH-SY5Y cells. Using the same *in vitro* model, we also determined the neuroprotective effects of these derivates against the toxicity caused by 3-nitropropionic acid (3-NP), a neurotoxin used to mimic pathological features of HD in mice and rats. Among the new arylpiperazine derivatives, we selected LQFM181 (**3**) to evaluate its *in vivo* antioxidant activity against the oxidative damage, locomotor behavior and memory dysfunction elicited by 3-NP in mice.

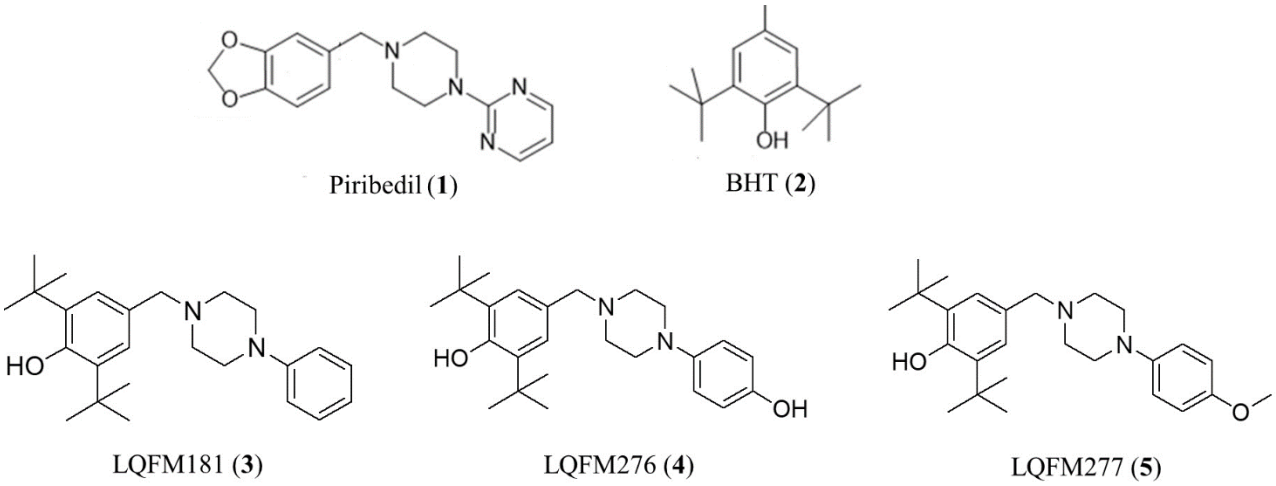

Figure 1: Chemical structures of piribedil (**1**), BHT (**2**), LQFM181 (**3**), LQFM276 (**4**) and LQFM277 (**5**) compounds.

2. Experimental Section

2.1 General procedure for the preparation of compounds

A solution of the 3,5-di-*tert*-butil-4-hydroxybenzaldehyde (**6**, Fig. 2) (234 mg, 1.0 mmol) and N-arylpiperazines (**7, 8 or 9**, Fig. 2) 1.0 mmol) in 5 mL of methanol was adjusted to pH 5.0 by

dropwise addition of concentrated acetic acid. In turn, $NaCNBH_3$ (63 mg, 1 mmol) was added and the resultant mixture stirred at 65 ºC for 2 h. Then the solvent under reduced pressure and the residue was partitioned between water and CH_2Cl_2. The combined organic layers were dried with Na_2SO_4, concentrated in vacuum, and the crude product was purified by column chromatography (SiO_2, hexane/AcOEt = 90:10) to offer (**3-5**) compounds.

2.1.1 Synthesis of 2,6-di-*tert*-butyl-4-((4-phenylpiperazin-1-yl)methyl)phenol (3) - LQFM181

Compound (**3**) was obtained (285 mg, 75%), as a white solid; mp = 180°C and Rf = 0.80 (hexane: AcOEt– 70:30). IR max (KBr) cm^{-1}: 3620 (υ OH), 3055 (υ C-H), 2897 (υ C-H), 1596 (υ C=C) (Fig. S1, Supplementary material). ^{1}H NMR (500.13 MHz) $CDCl_3$/TMS (δ): 7.25 (2H, *dd*, *J*=8.5 and 7.4, H10' and 12'), 7.16 (2H, *s*, H2 and 6), 6.92 (2H, *m*, H9' and 13'), 6.85 (1H, *t*, H11'), 5.18 (1H, *s*, C4-OH), 3.59 (2H, *m*, H1'), 3.27 (4H, *m*, H4' and 6'), 2.70 (4H, *s*, H3' and 7'), 1.59 (1H, *s*, C11'-OH), 1.44 (18H, *s*, H7 and 8) (Fig. S2 and Table 1, Supplementary material). ^{13}C NMR (125.76 MHz) $CDCl_3$/TMS (δ): 153.0 (C-4), 149.5 (C-8'), 145.8 (C-11'), 135.6 (C-3 and 5), 126.0 (C-1, 2 and 6), 118.3 (C-10' and 12'), 115.8 (C-9' and 13'), 63.0 (C-1'), 52.9 (C-3' and 7'), 50.6 (C-4' and 6'), 34.4 (C-9 and 10), 30.4 (C-7 and 8) (Fig. S3-5 and Table 1, Supplementary material). HRMS $[M+H]^+$ calculated for $C_{25}H_{36}N_2O$: 381.2906; found: 381.2845, Erro = -3.94 ppm (Fig. S6, Supplementary material).

2.1.2 Synthesis of for 2,6-di-*tert*-butyl-4-((4-(4-hydroxyphenyl)piperazin-1-yl)methyl)phenol (4) – LQFM276

Compound (**4**) was obtained (178 mg, 45%), as a white solid; mp = 162°C and Rf = 0.65 (hexane:AcOEt - 70:30). IR max (KBr) cm^{-1}: 3628 (υ OH), 3500-300 (υ OH), 3011 (υ C-H), 2955 (υ C-H), 1509 (υ C=C), 819 (υ Ar 1,4) (Fig. S7, Supplementary material). ^{1}H NMR (500.13 MHz) $CDCl_3$/TMS (δ): 7.12 (2H, *s*, H2 and 6), 6.84 (2H, *m*, H10' and 12'), 6.74 (2H, *m*, H9' and 13'), 5.14 (1H, *s*, OH), 3.53 (2H, *s*, H1'), 3.10 (4H, *m*, H4' and 6'), 2.64 (4H, *m*, H3' and 7'), 1.45 (2H, *s*, H7

and 8) (Fig. S8 and Table 2, Supplementary material). ^{13}C NMR (125.76 MHz) $CDCl_3$/TMS (δ): 153.2 (C-4), 151.2 (C-8'), 135.8 (C-3 and 5), 129.1 (C-10' and 12'), 126.3 (C-1), 126.3 (C-2 and 6), 119.9 (C-11'), 116.2 (C-9' and 13'), 62.9 (C-1'), 52.6 (C-3' and 7'), 48.8 (C-4' and 6'), 34.3 (C-7 and 8), 30.4 (C-9 and 10) (Fig. S9-10 and Table 2, Supplementary material). HRMS $[M+H]^+$ calculated for $C_{25}H_{37}N_2O_2$: 397.2855; found: 397.281, Erro = 11.00 ppm (Fig. S11, Supplementary material).

2.1.3 Synthesis of 2,6-di-*tert*-butyl-4-((4-(4-methoxyphenyl)piperazin-1-yl)methyl)phenol (5) – LQFM277

Compound (**5**) was obtained (172 mg, 42%), as a white solid; mp = 132°C and Rf = 0.64 (hexane:AcOET - 70:30) (Fig. S12, Supplementary material). IR max (KBr) cm^{-1}: 3635 (υ OH), 2996 (υ C-H), 2957 (υ C-H), 1516 (υ C=C), 828 (υ Ar 1,4). ^1H NMR (500.13 MHz) $CDCl_3$/TMS (δ): 7.15 (1H, *s*, H2 and 6), 6.90 (2H, *m*, H10' and 12'), 6.83 (2H, *m*, H9' and 13'), 5.19 (1H, *s*, OH), 3.77 (3H, *s*, H14'), 3.61 (2H, *s*, H1'), 3.16 (2H, *s*, H4' and 6'), 2.71 (2H, *s*, H3' and 7'), 1.45 (18H, *s*, H7 and 8) (Fig. S13 and Table 3, Supplementary material). ^{13}C NMR (125.76 MHz) $CDCl_3$/TMS (δ): 153.9 (C-8'), 153.3 (C-4), 145.6 (C-11'), 135.6 (C-3 and 5), 126.5 (C-1), 126.5 (C-2 and 6), 118.4 (C-10' and 12'), 114.5 (C-9' and 13'), 62.9 (C-1'), 55.6 (C-14'), 52.7 (C-3' and 7'), 50.1 (C-4' and 6'), 34.3 (C-9 and 10), 30.9 (C-7 and 8) (Fig. S14-15 and Table 3, Supplementary material). HRMS $[M+H]^+$ calculated for $C_{26}H_{39}N_2O_2$: 411.3012; found: 411.3000, Erro = 2.2 ppm (Fig. S16, Supplementary material).

2.2 *In vitro* Tests

2.2.1 Cell culture

Human neuronal SH-SY5Y cells were obtained from the Lombardy and Emilia Romagna Experimental Zootechnic Institute (Italy). These cells were cultured routinely in Dulbecco's Modified Eagle Medium with phenol red, supplemented with 10% fetal bovine serum, 2 mM L-glutamine, 50

U/mL penicillin, and 50 μg/mL streptomycin at 37°C in a humidified incubator with 5% CO_2. To maintain consistency, SH-SY5Y cells were utilized for experiments before passage 12 to prevent alterations in phenotype and cellular aging. Compounds **(3-5**) were dissolved in dimethyl sulfoxide (DMSO) at a concentration of 20 mM. Further dilutions of these stock solutions were made in complete medium to achieve desired compounds concentrations, with a maximum DMSO concentration of 0.1%.

2.2.2 Neuronal Viability

Neuronal viability was assessed by measuring the reduction of 3-(4,5-dimethylthiazol-2-yl)-2,5-diphenyl) tetrazole bromide (MTT) to its insoluble formazan, following the method described by Guardigni et al. (2023) [34]. SH-SY5Y cells were seeded in a 96-well plate at a density of 2×10^4 cells per well, incubated for 24 hours, and then treated with various concentrations of the compounds (**3-5**) ranging from 1.25 to 40 μM for 24 hours at 37°C in 5% CO_2. Afterward, the treatment medium was replaced with MTT in Hank's Balanced Salt Solution (HBSS) at a concentration of 0.5 mg/mL for 2 hours at 37°C in 5% CO_2. Following a wash with HBSS, formazan crystals were dissolved in isopropanol. The quantity of formazan was measured at 570 nm with a reference filter at 690 nm using the VICTOR™ X3 multilabel plate reader (PerkinElmer, Waltham, MA, USA). The data are presented as a percentage relative to untreated cells.

2.2.3 Antioxidant activity

The total antioxidant activity (TAA) of compounds **(3-5**) was assessed in SH-SY5Y cells following the method described by Ortiz et al. (2020) [35]. Initially, cells were seeded in a 96-well plate at a density of 3×10^4 cells per well, cultured for 24 hours, and then treated with the fluorescent probe H_2DCF-DA (10 μg/mL) for 30 minutes at room temperature. After incubation, cells were treated with compounds (**3-5**) at a concentration of 5 μM, along with tert-butyl hydroperoxide (t-BuOOH) (100 μM), for 30 minutes. The intracellular ROS formation was measured using a

VICTOR™ X3 multilabel plate reader (excitation at 485 nm and emission at 535 nm), and data were presented as the percentage inhibition of ROS formation induced by t-BuOOH.

Additionally, the TAA was determined in both cytosolic and membrane-enriched fractions, following the protocol described by Pruccoli et al. (2020) [24]. SH-SY5Y cells were seeded in culture dishes at a density of 4×10^6 cells per dish and cultured for 24 hours at 37°C in 5% CO_2. After the incubation period, cells were treated with compounds (**3-5**) at a concentration of 5 μM for 2 hours. Following washing with cold phosphate-buffered saline (PBS), cells were collected and centrifuged, and the resulting pellet was reconstituted in 0.05% Triton X-100. After homogenization and incubation at 4°C, cytosolic and membrane-enriched fractions were separated by centrifugation. TAA in cell fractions was determined by the discoloration of the radical cation of $ABTS^{\bullet+}$, with absorbance measured at 740 nm. Data were compared with the concentration-response curve of a standard antioxidant, such as Trolox, and expressed as μmol of Trolox Equivalent Antioxidant Activity per milligram of protein (μmolTE/mg protein).

2.2.4 Neuroprotective activity

SH-SY5Y cells were seeded in a 96 well plate at 3×10^4 cells/well, incubated for 24 h, and subsequently treated with (**3-5**) compounds (5 μM) and 3-NP acid (20 mM) for 24 h. The neuronal viability was measured by using the MTT assay as previously described [37]. Data are expressed as a percentage of neurotoxicity versus untreated cells.

2.3 *In vivo* Tests

2.3.1 Animals

Experiments were conducted using male *Swiss* mice (25 – 30 g) about two months old. Animals were maintained at a stable temperature of 22 ± 2 °C and a controlled 12 hours light/dark cycle, with free access to food and water. All manipulations were carried out between 08:00 and 16:00 hours. All the protocols and experimentations were carried out in accordance with the

Regulations of the National Council for the Control of Animal Experimentation (CONCEA), complying with the ARRIVE guidelines and in accordance with the National Research Council's Guide for the Care and Use of Laboratory Animals and approved by the local Ethics in Research Committee of the Federal University of Goiás (UFG) (protocol number 053/2016).

2.3.2 Experimental design

The animals were randomized into five groups (N= 10): Control, 3-NP 15 mg/kg (3-NP), LQFM181 (**3**) 10 mg/kg v.o. (LQFM10), LQFM181 (**3**) 25 mg/kg v.o. (LQFM25) and LQFM181 (**3**) 50 mg/kg v.o. (LQFM50). The animals received in the first treatment, daily oral administrations of LQFM181 (**3**) (or ethanol solution 1%, for control and 3-NP groups) for a period of thirty-one days, and in the second treatment, the animals received intraperitoneal administrations of 3-NP on alternate days (or saline solution 0.9% for control group) for the same period. The interval between the treatments was of one hour. The dose of 3-NP as well as the type of exposure was based on the previous work of Abdelfattah et al. (2020) [38]. At the end of the treatment, the behavioral tests were performed, and later, the animals were euthanized for the removal of tissues for biochemical analysis.

2.3.3 Behavioral tests

2.3.3.1 Cylinder Climb Test (CCT)

Locomotor activity was assessed using the cylinder climb test (CCT), a method introduced to evaluate the animal's capacity to climb backward within a cylindrical tube. This procedure, outlined by Brito et al. (2018) [23], entailed initially placing the animals horizontally inside the tube. Subsequently, as they moved towards the opposite end, the tube was repositioned vertically. The climbing behavior was then observed and quantified for a duration of 30 seconds. This test served to elucidate the animals' climbing tendencies and locomotor skills.

2.3.3.2 Open field Test (OF)

Exploratory behavior was evaluated following the methodology delineated by Antiorio et al. (2022) [39]. Animals were placed individually in the center of the open field apparatus, which was divided into nine squares. The number of segments traversed by each animal, adhering to the four-paw criterion, was tallied during a 5-minute session. This method enabled the quantification of the animals' exploratory activity within the specified area.

2.3.3.3 Rotarod Test (RR)

Motor abilities were evaluated on the 32nd day of the experiment. Throughout the training period, the creatures were placed in the device at a speed of 10 rotations per minute (rpm) for 5 minutes. In the retention phase, the rotarod was set to accelerate from 5 rpm to about 50 rpm, and the duration the animals stayed on the device was noted, with a maximum of 5 minutes. During all phases of testing, the time it took, measured in seconds, for the animals to fall off the rotarod was recorded, following the methodology outlined by Collenberg et al. (2019) [40].

2.3.3.4 Step-down Avoidance Test (SDPAT)

To evaluate nonspatial long-term memory, we followed the procedure outlined by Campos et al. (2022) [41]. The experimental arrangement consisted of a solitary enclosure furnished with a stable platform and a metallic mesh linked to a shock generator. On day 32, during the acquisition stage, mice were positioned on the stable platform. As soon as they set foot on the mesh with all four paws, they experienced a 0.5 mA/s electric shock. The duration it took for the mice to commence descending onto the mesh was documented during the acquisition phase. The retention phase occurred on day 33, 24 hours post the acquisition phase. During this phase, the mice were once again positioned on the stable platform, but no electric shock was administered upon descending onto the mesh. Successful learning was gauged by an increase in the time it took to transfer during the retention trial. Consequently, short transfer times suggested poorer retention of the memory.

2.4 Tissue collection

Twenty-four hours following the final behavioral test, the animals were anesthetized intraperitoneally using ketamine and xylazine hydrochloride. Subsequently, they were euthanized through decapitation, and the striatum was carefully dissected and isolated. The extracted samples were homogenized in 50 mM potassium phosphate buffer (KPB) with a pH of 7.4, using a ratio of 1 part sample to 6 parts buffer (w/v). The resulting homogenate (HT) was then subjected to centrifugation at 8000 x g for 10 minutes, producing the low-speed supernatant (S1). Both the HT and S1 fractions were preserved and utilized for the subsequent assay procedures.

2.5 Biochemical assays

2.5.1 Cholinesterase (ChE) activity

Cholinesterase (ChE) enzyme levels were analyzed using the technique outlined by Okoh et al. (2024) [15]. The S1 fractions underwent a process where they were combined with 1 mM DTNB, then enzymatic reaction was initiated with the addition of 1 mM ATCh and BTCh as substrates for AChE and BChE, respectively. Spectrophotometric measurements were taken at 412 nm over 5 minutes to assess enzyme activities. The activities are expressed in terms of μmol ACTh/min/mg protein and μmol BCTh/min/mg protein for AChE and BChE, respectively.

2.5.2 Lipid peroxidation (LPO) levels

The thiobarbituric acid reactive substances (TBARs) method was utilized to gauge the levels of lipid peroxidation (LPO), following the procedure detailed by Okoh et al. (2024) [15]. The HT fractions underwent incubation with thiobarbituric acid, trichloroacetic acid (at pH 3.4), and SDS at 95 °C for 60 minutes. The resulting reaction product was quantified spectrophotometrically at 532 nm. The analysis of the results involved constructing an MDA curve, with the data presented as malondialdehyde (MDA) equivalents in nmol/mg protein.

2.5.3 Carbonylated protein (CP) levels

Protein carbonyl derivatives were measured employing the technique described by Campos et al. (2022) [41]. The HT fractions underwent incubation with 2 mol/L HCl-prepared DNPH for 1 hour, with intermittent vortexing every 15 minutes. Following the sample denaturation, the resultant product was spectrophotometrically assessed at 370 nm, and the results were expressed as nmol of carbonyl content per mg protein.

2.5.4 Superoxide dismutase (SOD) activity

The evaluation of SOD activity followed the methodology of Campos et al. (2022) [41]. The S1 fractions of the samples were subjected to incubation with 60 mM epinephrine bitartrate and a glycine buffer (50 mM, pH 10). The spectrophotometric measurement of the resulting solution's color intensity was conducted at 480 nm. The enzymatic activity was quantified and presented in units (U) of SOD per milligram of protein.

2.5.5 Catalase (CAT) activity

CAT activity was evaluated by measuring the breakdown of H_2O_2, following to the procedure delineated by Okoh et al. (2024) [15]. The S1 fractions underwent incubation with 86 mM H2O2 and sodium phosphate buffer (pH 7.0), and the resulting reaction was assayed spectrophotometrically at 240 nm. The enzymatic activity was determined and represented in units (U) of CAT per milligram of protein.

2.5.6 Succinate dehydrogenase (SDH) activity – Complex II

The method for estimating SDH involves the conversion of succinic acid into fumaric acid in the presence of an electron acceptor, potassium ferricyanide, as per the protocol outlined by Brondani et al. (2023) [42]. The mitochondrial suspension was introduced into a reaction mixture comprising phosphate buffer (0.2 M, pH 7.8), succinic acid (0.6 M, pH 7.8), 1% (w/v) BSA, and potassium

ferricyanide (0.3 M). Succinate dehydrogenase activity was determined by measuring the decrease in absorbance at 420 nm over 3 minutes, with water used as a blank. Results were expressed in nmol succinate oxidized per minute per milligram of protein.

2.5.7 Protein content determination

The total protein concentration of the samples was determined using the Bradford's method described by Campos et al. (2022) [41].

2.6 Data presentation and statistical analysis

All experimental results are presented as the mean (± standard deviation) ± standard error of the mean (SEM). Statistical analyses were conducted using one-way ANOVA or two-way ANOVA, followed by Tukey's multiple comparisons test. A significance level of $p < 0.05$ was considered statistically significant. Data analysis was performed using GraphPad Prism 8.0 software (San Diego, CA, USA) available at https://www.graphpad.com.

3. Results and Discussion

3.1 Chemistry

Figure 2A illustrates the structural design of LQFM181 (**3**), LQFM276 (**4**), and LQFM277 (**5**) derived from piribedil (**1**) and BHT (**2**) lead compounds. Figure 2B depicts the synthetic route for obtaining LQFM181 (**3**), LQFM276 (**4**), and LQFM277 (**5**). As indicated, LQFM181 (**3**), LQFM276 (**4**), and LQFM277 (**5**) were synthesized via reductive amination reaction [43], yielding 75%, 45%, and 42%, respectively, in a single step. These final compounds consist of a fusion of a BHT molecule and an arylpiperazine moiety. The structural difference among them lies in the W position of the benzene ring of the arylpiperazine moiety: LQFM276 (**4**) features an OH group, LQFM277 (**5**) contains an OCH3 group, and LQFM181 (**3**) possesses a hydrogen atom. This structural variation affects the polarity of the molecules, with LQFM181 **(3)** showing a lower degree. Such variability

could impact the molecules' affinity levels with cellular lipid barriers. This hypothesis appears supported by *in silico* ADME parameters and subsequent *in vitro* results, as detailed following the findings of this study.

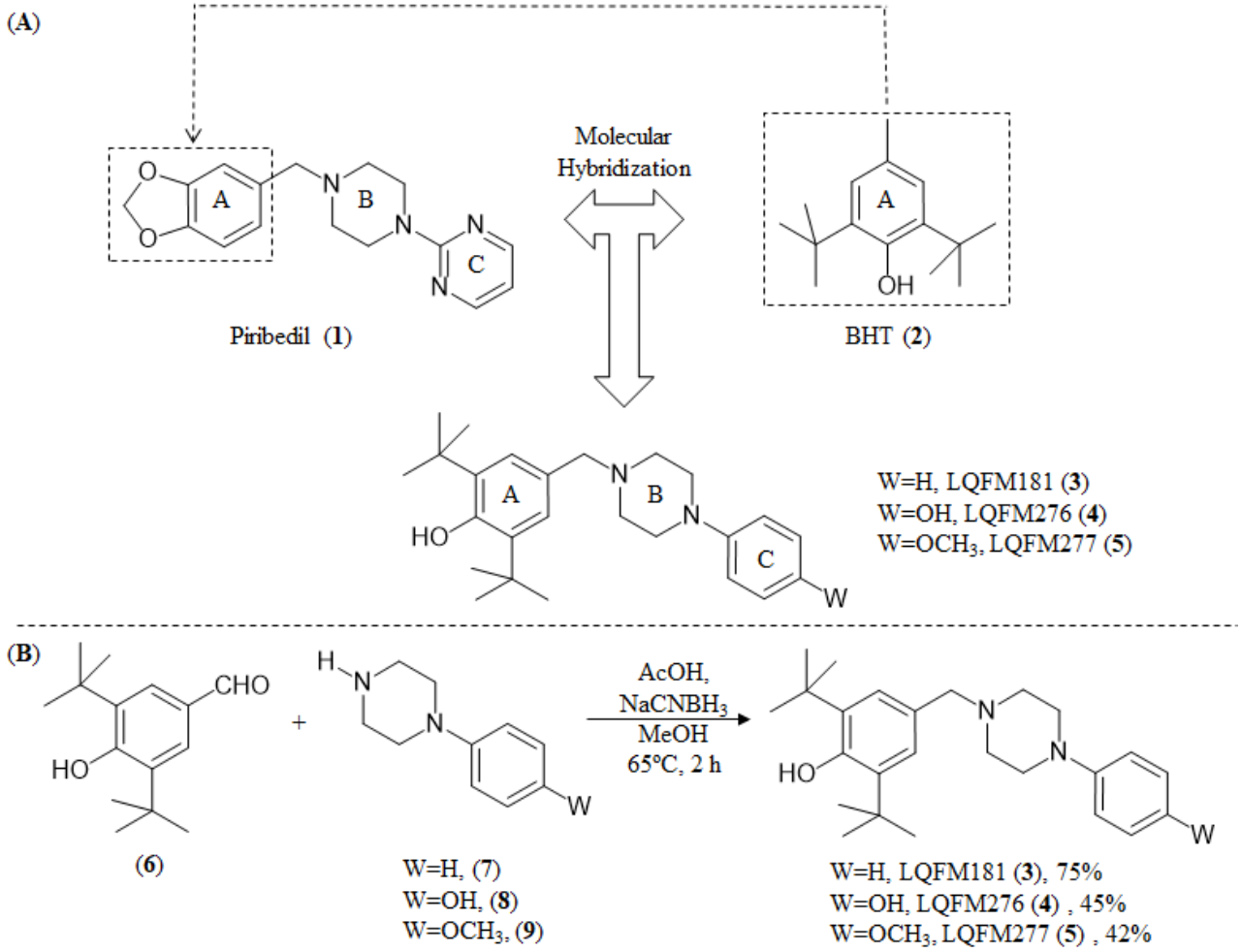

Figure 2: (**A**) Structural design of LQFM181 (**3**), LQFM276 (**4**) and LQFM277 (**5**) from piribedil (**1**) and BHT (**2**) lead compounds. (**B**) Synthetic route for obtention of LQFM181 (**3**), LQFM276 (**4**) and LQFM277 (**5**).

3.2 *In vitro* Studies

3.2.1 Neurotoxicity, *in silico* ADME and antioxidant activity

The *in vitro* neurotoxicity effects of BHT, piribedil, LQFM181 (**3**), LQFM276 (**4**), and LQFM277 (**5**) were assessed at various concentrations (1.25 - 40 μM) in human neuronal SH-SY5Y cells after 24 hours of treatment using the MTT assay. Notably, none of the compounds exhibited any

detectable neurotoxic effects at the highest concentration employed (data not shown). Additionally, we determined the *in silico* ADME (Absorption, Distribution, Metabolism, and Excretion) parameters of the compounds using SwissADME program (Swiss Institute of Bioinformatics - © 2023). The results indicated favorable properties of compounds for oral absorption as well as permeation of the blood-brain barrier. Furthermore, the adherence to Lipinski's rule of five suggested the potential druggability of the selected compounds. It's important to note that LQFM181 exhibited a decreased value of polar surface area (PSA) compared to LQFM276 and LQFM277 (Supplementary File). This finding indicates that it may have better permeability across biological barriers, which was corroborated by *in vitro* tests where LQFM181 showed the best ability to exert antioxidant activity in the cytoplasm of SH-SY5Y cells (Table 1).

Regarding the total antioxidant activity (TAA) of BHT (**2**), piribedil (**1**), LQFM181 (**3**), LQFM276 (**4**), and LQFM277 (**5**), the results are presented in Table 1. It is noteworthy that, except for piribedil (**1**), all other compounds demonstrated the capacity to scavenge ABTS radicals. Specifically, the compounds exhibited the following order of increasing antioxidant activity: BHT < LQFM181 < LQFM276 < LQFM277. In parallel, the TAA of the (**3-5**) studied compounds was evaluated in neuronal SH-SY5Y cells against the reactive oxygen species (ROS) formation induced by t-BuOOH. After 30 min of treatment with (**3-5**) compounds (5 μM) and t-BuOOH (100 μM), the ROS formation was detected using the fluorescent probe H_2DCF-DA. As shown in Table 1, BHT (**2**), LQFM181 (**3**), LQFM276 (**4**), and LQFM277 (**5**) showed the ability to reduce the ROS formation in neuronal SH-SY5Y cells. In particular, LQFM181 (**3**), LQFM276 (**4**) and LQFM277 (**5**) TAA were higher than BHT (**2**). In similar experimental conditions, piribedil (**1**) did not show TAA in neuronal SH-SY5Y cells, confirming the results with ABTS radicals.

Table 1. Antioxidant activity of the compounds in neuronal SH-SY5Y cells[a]

Compound	TAA (µmolTE/mL)[b]	TAA vs t-BOOH in SH-SY5Y cells[c]	TAA in SH-SY5Y cells (µmolTE/mg of protein)[d]	
			Membrane	Cytoplasm
Control	------	-------	2±0.1	31±2.9
BHT	26±5	43±24	5±0.7**	38±2.3*
piribedil	In	2±11	Nd	Nd
LQFM181	52±11	61±13	5±0.6**	50±5**§§
LQFM276	65±18	88±9	6±0.2**	34±0.9
LQFM277	83±5	61±12	8±0.5**	35±2.12

[a]Data are represented as mean ± SD of three independent experiments; [b]TAA of the compounds is expressed as µmol TE; [c]TAA is expressed as % inhibition of ROS formation induced by t-BuOOH in SH-SY5Y cells after a simultaneous treatment with the compound (5 µM) and t-BOOH (100 µM); [d]TAA of the compounds is expressed as µmol TE for mg of membrane or cytoplasmic protein of SH-SY5Y cells (*$p<0.05$ and **$p<0.01$ versus untreated cells (control); §§$p<0.01$ versus cells treated with BHT; at one-way ANOVA followed by post hoc Tukey's test). In: inactive; Nd: not determined.

The assessment of TAA was extended to both cytosolic and membrane fractions of neuronal SH-SY5Y cells treated with 5 µM of the compounds for 2 hours, using the ABTS assay. This approach allowed us to elucidate the cellular uptake of the (**3-5**) compounds and their capacity to counteract free radicals at distinct subcellular levels. Specifically, the membrane fractions obtained from neuronal SH-SY5Y cells treated with BHT (**2**), LQFM181 (**3**), LQFM276 (**4**), and LQFM277 (**5**) exhibited a significant increase in TAA in comparison to untreated cells. By contrast to LQFM276 (**4**) and LQFM277 (**5**), only BHT (**2**) and LQFM181 (**3**) showed a significant increase in TAA for the cytosolic fractions suggesting their ability to cross neuronal membrane and exert the antioxidant

activity in the cytoplasm too (Table 1). Notably, cytoplasm TAA of the cells treated with LQFM181 (**3**) was significantly higher than those treated with BTH (**2**). Piribedil (**1**) TAA in neuronal SH-SY5Y cells was not evaluated because it did not show antioxidant activity against t-BuOOH. This outcome underscores the different subcellular effects of these compounds in addressing oxidative stress.

3.2.2 Neuroprotective activity

The neuroprotective effects of the compounds against the neurotoxicity induced by 3-NP in neuronal SH-SY5Y cells were then assessed using MTT assay. As illustrated in Figure 3, treatment with LQFM181 (**3**), LQFM276 (**4**), and LQFM277 (**5**) at a concentration of 5 μM significantly reduced the neurotoxic effects induced by 24 hours of exposure to 3-NP acid. Among the tested compounds, LQFM181 (**3**) exhibited the highest level of neuroprotection, showing a remarkable 55% inhibition of neurotoxicity. Conversely, BHT (2) and piribedil (1) did not demonstrate significant neuroprotective effects in the same experimental conditions. These results provide compelling evidence for the considerable neuroprotective potential of LQFM181 (**3**), reinforcing its promising role in the protection against neurotoxicity induced by 3-NP acid in neuronal SH-SY5Y cells.

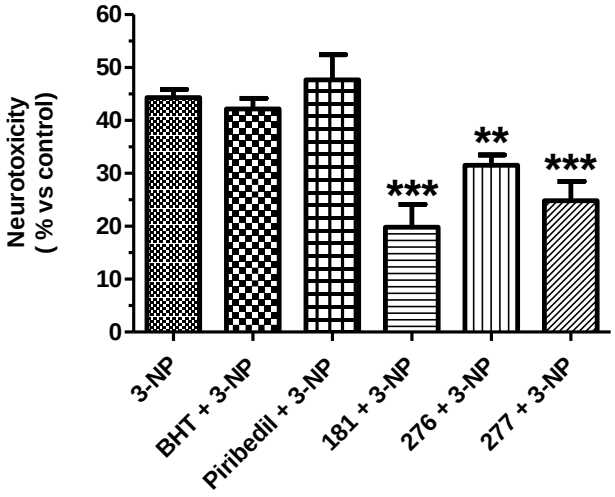

Figure 3. Effects of BHT (**2**), piribedil (**1**), LQFM181 (**3**), LQFM276 (**4**) and LQFM277 (**5**) compounds against 3-NP acid induced neurotoxicity in neuronal SH-SY5Y cells, treated with compounds (5 μM) and 3-NP (20 mM) for 24 h. Data are reported as mean ± SEM of at least three

independent experiments (**p < 0.01 and ***p < 0.001 versus untreated cells at one-way ANOVA with the Tukey's post-hoc test).

Among the (**3-5**) studied compounds, LQFM181 (**3**) showed favorable ADME Properties (Table 4, Supplementary material) as well as the best profile of antioxidant and neuroprotective activity in neuronal SH-SY5Y cells. On the basis of this evidence, we therefore selected LQFM181 (**3**) for subsequent *in vivo* experiments.

3.3 *In vivo* studies

3.3.1 Behavioral evaluation

The *in vivo* experiments were conducted with male Swiss mice, utilizing the mitochondrial toxin 3-NP known to induce neurotoxicity in animals and humans, thereby mimicking HD-like symptoms [44,45]. This toxin not only brings about changes in locomotor and cognitive systems but also disrupts the cholinergic system, leading to OS [46-49]. In light of these observations, our study involved comprehensive behavioral and biochemical assessments to gauge motor, cognitive, and OS parameters in mice treated with 3-NP. The primary objective was to ascertain whether LQFM181 (**3**) could effectively mitigate the detrimental effects induced by this toxin. In this regard, we treated the mice with LQFM181 (**3**) at different dose levels, 10 mg/kg (LQFM10), 25 mg/kg (LQFM25), and 50 mg/kg (LQFM50) before treating them with 3-NP. We did not include the piribedil and BHT compounds in *in vivo* study due to their lack of neuroprotective effects *in vitro*, which aligns with ethical guidelines that aim to minimize the number of animals used in research.

We employed the chimney test, a behavioral evaluation involving the animal's ability to climb backward within a cylindrical tube. Starting from the first day, all groups receiving 3-NP exhibited an increased climbing time compared to the control group ($p < 0.05$). However, from the fifteenth day onward until the conclusion of the treatments, only the 3-NP group sustained a significant difference from the control group ($p < 0.05$), while the groups receiving LQFM181 (**3**), at all tested doses, effectively restored the locomotor impairment caused by 3-NP (Figure 4 A). Additionally, the

rota rod test was utilized to assess animal motor skills, revealing that the 3-NP group exhibited reduced motor activity resistance in comparison to the control group. Notably, treatment with LQFM181 (**3**) at all doses led to a substantial increase in locomotor activity compared to the 3-NP group ($p = 0.0001$) (Figure 4B). Similarly, the exploratory activity of mice, as measured by the number of crossings in the open field test, indicated reduced locomotor activity in the 3-NP group. Encouragingly, the administration of LQFM181 (**3**) effectively counteracted the motor damage induced by the toxin (Figure 4C). The results from all the conducted tests strongly support the protective effects of LQFM181 (**3**) against the motor impairments caused by 3-NP.

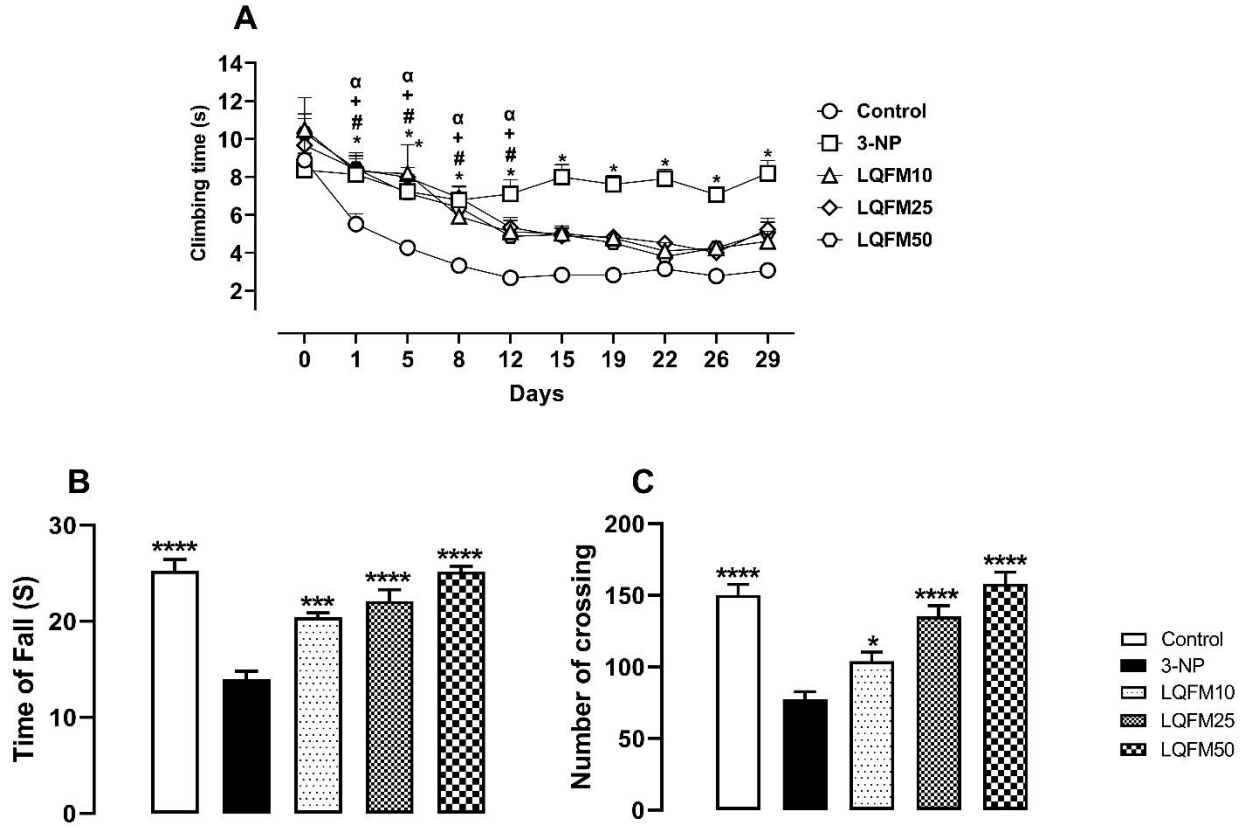

Figure 4: Effect of LQFM181 (**3**) treatments in time of climbing (A), time of fall (B) and crossing frequency (C) on locomotor impairment induced by 3-NP in mice. Data are represented as the mean ± SEM of 10 animals per group. Statistical analysis was performed using two-way ANOVA for chimney test (Figure A) and one-way ANOVA for rota rod and open field tests (Figures B and C). In both cases, analyses are followed by Tukey's post-hoc test.

$^{\#, \sigma, \varepsilon, +}$ $p < 0.05$ when compared to the control group;

* $p < 0.05$; *** $p < 0.001$, **** $p < 0.0001$ when compared to the 3-NP group

Furthermore, in addition to inducing locomotor impairment, 3-NP has been observed to inflict memory damage by eliciting selective striatal neuropathology, effectively mirroring the neuropathological features of HD [50]. We conducted the step-down avoidance test to comprehensively evaluate this memory impairment caused by 3-NP. The results from this test demonstrated that administration of all three doses of LQFM181 (**3**) significantly increased the latency time of the mice during the step-down motion, providing clear evidence of the protective effect of LQFM181 (**3**) against the memory damage induced by 3-NP (Figure 5).

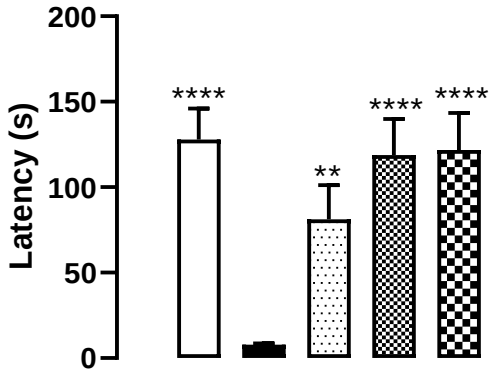

Figure 5: Effect of LQFM181 (**3**) treatments in the retention phase (24 h after the training phase) on 3-NP induced memory impairment in the step-down avoidance test in mice. Data are represented as mean ± SEM. for n = 16 to 18 animals per group. Statistical analysis was performed using one-way ANOVA followed by Tukey's test. ** $p < 0.01$, **** $p < 0.0001$, when compared to the 3-NP group.

The striatum was chosen as the brain region of interest for the biochemical assessments due to 3-NP's demonstrated propensity to rapidly induce striatal lesions following administration. The neurotoxicity of 3-NP involves the irreversible inhibition of mitochondria complex II, disrupting the electron transport cascade and oxidative phosphorylation. This disruption leads to a cellular energy deficit [51,52]. Furthermore, 3-NP exposure reduces ATP production, promotes weight loss, and

causes dysfunction in the cholinergic system. It also increases levels of LPO and protein oxidation, simultaneously decreasing the activity of antioxidant enzymes [49,53,54].

Additionally, the observed alterations in locomotor and motor behavior can be attributed to the specific impact of 3-NP on the striatum [48]. Furthermore, it is well-established that the cognitive impairment caused by 3-NP is closely associated with dysfunction in the cholinergic system, resulting in an increase in cholinesterase activity [48,55].

Our study revealed that treatment with LQFM181 (**3**) inhibited the increase in acetylcholinesterase and butyrylcholinesterase activities induced by 3-NP (Table 2). This observation holds significant importance as it aligns perfectly with the results of the step-down avoidance test, strongly suggesting that the protection conferred by LQFM181 (**3**) against memory impairment involves its modulatory action on the cholinergic system. This interplay between LQFM181 (**3**) and the cholinergic system could provide a mechanistic explanation for the observed memory-preserving effects of LQFM181 (**3**). In addition, the presence of arylpiperazine moiety in the LQFM181 (**3**) may explain its anticholinesterase effect, since this action is already described for compounds having piperazine group [56,57].

3.3.2 Oxidative Damage Evaluation

The exposure of mice to 3-NP also resulted in weight loss (Figure 6) and inhibited SDH activity (Table 2). Previous studies indicate that weight loss can be caused by various factors including the inhibition of the SDH enzyme in the Krebs cycle, resulting in a depletion of ATP, the brain's main energy source, and OS [58,59]. SDH inhibition disrupts electron transport, leading to an increase in free radical formation and a decrease in ATP production, ultimately contributing to weight loss [60-62]. However, treatment with three different doses of LQFM181 (**3**) effectively protected against 3-NP-induced weight loss by restoring SDH activity. Mitochondrial dysfunction is a characteristic of neurodegeneration [7], and the activity of the succinate dehydrogenase is a marker of mitochondrial function [63]. In this context, restoration of weight loss and SDH activity by

LQFM181 (**3**) treatment, confirmed its protective effect. This protective effect is likely due to the antioxidant properties of LQFM181 (**3**), since this effect is described to alleviate the mitochondrial dysfunction induced by 3-NP [64].

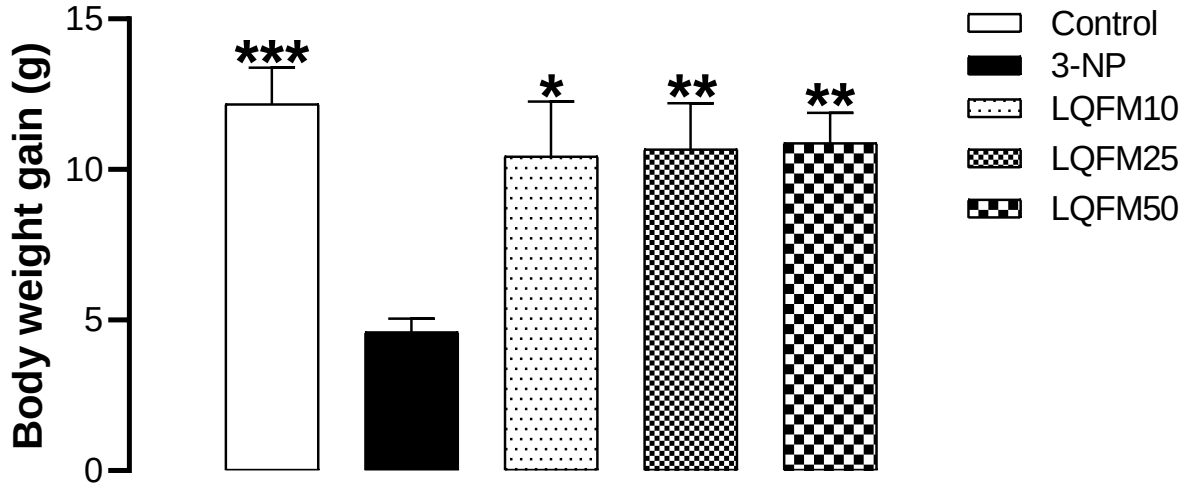

Figure 6: Effect of LQFM181 (**3**) treatments in the body weight loss induced by 3-NP in mice. Data are represented as mean ± SEM. for n = 16 to 18 animals per group. Statistical analysis was performed using one-way ANOVA followed by Tukey's test. * $p < 0.05$, ** $p < 0.01$, *** $p < 0.001$, when compared to the 3-NP group.

Table 2. Effects of different doses of LQFM181 (**3**) on striatum SDH, AChE, BChE, SOD and CAT activities and the MDA and PC levels in 3-NP-treated mice.

	Control	3-NP	LQFM10	LQFM25	LQFM50
SDH	63.33 ± 4.40*	26.37 ± 2.26	46.62 ± 4.35*	46.69 ± 4.67*	61.69 ± 5.28*
AChE	2.07 ± 0.16*	5.71 ± 0.48	3.81 ± 0.45*	3.52 ± 0.20*	2.86 ± 0.22*
BChE	1.00 ± 0.19*	2.43 ± 0.06	1.51 ± 0.18*	1.28 ± 0.17*	1.25 ± 0.12*
SOD	35.45 ± 1.79*	13.65 ± 0.81	22.47 ± 0.70*	25.34 ± 0.76*	33.01 ± 1.99*
CAT	13.72 ± 1.16*	7.43 ± 0.36	11.53 ± 1.29*	12.76 ± 4.16*	17.50 ± 4.24*
MDA	6.28 ± 0.32*	9.81 ± 0.43	7.74 ± 0.24*	6.14 ± 0.20*	5.39 ± 0.29*
CP	1.17 ± 0.06*	2.75 ± 0.12	1.89 ± 0.09*	1.43 ± 0.05*	1.35 ± 0.07*

Values are presented as means ± SEM (n = 10) and analyzed by one-way ANOVA followed by post hoc Tukey's test. SDH (nmol of succinate oxidized/min/mg of protein), AChE (μmol ACTh/min/mg of protein), BChE (μmol BCTh/min/mg of protein) SOD (U/mg of protein) and CAT (U/mg of protein) activities, MDA (nmol/mg of protein) and PC (nmol/mg of protein) levels. * $p < 0.05$, when compared to 3-NP group.

In the final phase of the tests, the evaluation of OS in the mice's striatum yielded significant results. LQFM181 (**3**) was found to be remarkably effective in protecting against lipid peroxidation induced by 3-NP, as indicated by the measurement of TBARs and levels of CP. Notably, 3-NP led to an increase in the levels of these markers in both tests, but treatment with LQFM181 (**3**) at all tested doses successfully inhibited this increase (Table 2). This finding underscores the potent protective effect of LQFM181 (**3**) against the destruction of membrane lipids and the formation of end-products resulting from such LPO reactions, which are particularly detrimental to cellular health.

Furthermore, LQFM181 (**3**) exhibited the ability to counteract the decrease in activity of the SOD and CAT enzymes, which are integral components of the first-line antioxidant defense system

(Table 2). These enzymes play a crucial role in the cellular defense strategy against oxidative stress, akin to the function of antioxidant agents like LQFM181 (**3**). By inhibiting the decline in the activities of these enzymes caused by the toxin, LQFM181 (**3**) contributes to bolstering the overall antioxidant capacity of the system, further solidifying its potential as a robust neuroprotective agent.

Several molecules containing the piperazine nucleus have been developed as potent leads for treating AD, PD, depression, and other disorders [65]. The arylpiperazine moiety is found in a large number of bioactive molecules, exhibiting various activities, including anti-inflammatory, anticholinesterase, and cognition-enhancing effects [32, 56, 57, 65, 66]. Given that the arylpiperazine nucleus can be substituted at different chemical structures, offering flexibility for synthesizing numerous derivatives, we incorporated it into a molecule with significant antioxidant properties. This strategy increased antioxidant properties and enhanced the range of action of the arylpiperazine nucleus, creating a new compound with greater potential for treating NDs. Indeed, LQFM181 (**3**) demonstrated significant *in vitro* antioxidative effects, which were confirmed by *in vivo* tests. Furthermore, it exhibited other desirable characteristics for combating NDs, such as anti-cholinesterase activity and memory restoration.

Moreover, OS is recognized for its ability to activate various transcription factors implicated in inflammatory pathways, with inflammation induced by OS being a contributing factor to numerous chronic diseases [67]. In a recent study, Moreira et al. (2023) demonstrated that LQFM212, a piperazine derivative incorporating BHT in its chemical structure, attenuated TNF-α, IL-1β, IL-4, and IL-10 mediators in a model of neuroinflammation induced by lipopolysaccharide (LPS). Given this context, although we did not investigate the effects of LQFM181 (**3**) on neuroinflammation, it is plausible to suggest that LQFM181 (**3**) may similarly suppress neuroinflammation. However, this hypothesis warrants further investigation for confirmation.

Therefore, in line with polyphenols and marine compounds, which are currently being explored as potential new drugs for treating NDs due to their broad effects, including the suppression

of the OS, LQFM181 (**3**) emerges as a compound similar to them, positioning it as a new lead compound for the treatment of such diseases.

4. Conclusions

LQFM181 is a novel compound resulting from the fusion of an arylpiperazine nucleus with an antioxidant molecule that exhibits multiple neuroprotective actions. This study showed its broad neuroprotective effects, including antioxidative, anticholinesterase, and memory-restoring properties. Additionally, LQFM181 (**3**) demonstrated favorable characteristics for crossing biological barriers, having displayed significant antioxidant activity within the cytoplasm of SH-SY5Y cells. Consequently, LQFM181 (**3**) emerges as a promising candidate for further investigation into its neuroprotective potential, positioning it as a new therapeutic agent for neuroprotection. While the findings of this study support evidence of LQFM181 (**3**)'s neuroprotective effects, further research is required to explore additional pharmacological activities, such as its anti-inflammatory action. Moreover, comprehensive studies are needed to elucidate its pharmacokinetic properties.

Acknowledgements

The authors thank Conselho Nacional de Desenvolvimento Científico e Tecnológico for providing two scholarships for the completion of this study (protocol number 401454/2022-3).

References

[1] Gontijo, V., Viegas, F., Ortiz, C., de Freitas S., Matheus, D., Caio, M., 2019. Molecular hybridization as a tool in the design of multi-target directed drug candidates for neurodegenerative diseases. Current Neuropharmacology. 18,348-407. https://doi.org/10.2174/1385272823666191021124443.

[2] Lamptey RNL, Chaulagain B, Trivedi R, Gothwal A, Layek B, Singh J. A., 2022. Review of the Common Neurodegenerative Disorders: Current Therapeutic Approaches and the Potential Role of Nanotherapeutics. Int J Mol Sci. 23(3):1851. https://doi.org/10.3390/ijms23031851.

[3] Bulck, M., Sierra-Magro, A., Alarcon-Gil, J., Perez-Castillo, A., Morales-Garcia, J., 2019. Novel approaches for the treatment of Alzheimer's and Parkinson's disease. International Journal of Molecular Sciences. 20, 1-36. https://doi.org/10.3390/ijms20030719

[4] Sudhakar V, Richardson RM., 2019. Gene Therapy for Neurodegenerative Diseases. Neurotherapeutics. 16(1):166-175. https://doi.org/10.1007/s13311-018-00694-0.

[5] Gao C, Jiang J, Tan Y, Chen S., 2023. Microglia in neurodegenerative diseases: mechanism and potential therapeutic targets. Signal Transduct Target Ther. 8(1):359. https://doi.org/10.1038/s41392-023-01588-0

[6] Bahbah EI, Ghozy S, Attia MS, Negida A, Emran TB, Mitra S, Albadrani GM, Abdel-Daim MM, Uddin MS, Simal-Gandara J., 2021. Molecular Mechanisms of Astaxanthin as a Potential Neurotherapeutic Agent. Mar Drugs. 19(4):201. https://doi.org/10.3390/md19040201

[7] Gitler, A., Dhillon, P., Shorter, J., 2017. Neurodegenerative disease: models, mechanisms, and a new hope. Disease Models & Mechanisms. 10, 499-502. https://doi.org/ 10.1242/dmm.030205

[8] Lopez-Sanchez, C., Garcia-Martinez, V., Poejo, J., Garcia-Lopez, V., Salazar, J., Gutierrez-Merino, C., 2020. Early reactive A1 astrocytes induction by the neurotoxin 3-nitropropionic acid in rat brain. International Journal of Molecular Sciences Article. 21, 1-19. https://doi.org/ 10.3390/ijms21103609

[9] Su LJ, Zhang JH, Gomez H, Murugan R, Hong X, Xu D, Jiang F, Peng ZY., 2019. Reactive Oxygen Species-Induced Lipid Peroxidation in Apoptosis, Autophagy, and Ferroptosis. Oxid Med Cell Longev. 2019:5080843. https://doi.org/10.1155/2019/5080843

[10] Fujii, Junichi, Takujiro Homma, and Tsukasa Osaki., 2022. Superoxide Radicals in the Execution of Cell Death. Antioxidants 11(3): 501. https://doi.org/10.3390/antiox11030501

[11] Juan CA, Pérez de la Lastra JM, Plou FJ, Pérez-Lebeña E., 2021. The Chemistry of Reactive Oxygen Species (ROS) Revisited: Outlining Their Role in Biological Macromolecules (DNA, Lipids and Proteins) and Induced Pathologies. Int J Mol Sci. 22(9):4642. https://doi.org/10.3390/ijms22094642

[12] Islam F, Islam MM, Khan Meem AF, Nafady MH, Islam MR, Akter A, Mitra S, Alhumaydhi FA, Emran TB, Khusro A, Simal-Gandara J, Eftekhari A, Karimi F, Baghayeri M., 2022. Multifaceted role of polyphenols in the treatment and management of neurodegenerative diseases. Chemosphere. 307(Pt 3):136020. https://doi.org/10.1016/j.chemosphere.2022.136020

[13] Elfawy HA, Das B., 2019. Crosstalk between mitochondrial dysfunction, oxidative stress, and age-related neurodegenerative disease: Etiologies and therapeutic strategies. Life Sci. 218:165-184. https://doi.org/10.1016/j.lfs.2018.12.029

[14] Singh A, Kukreti R, Saso L, Kukreti S., 2019. Oxidative Stress: A Key Modulator in Neurodegenerative Diseases. Molecules. 24(8):1583. https://doi.org/10.3390/molecules24081583

[15] Okoh VI, Campos HM, Yasmin de Oliveira Ferreira P, Pereira RM, Souza Silva Y, Arruda EL, Pagliarani B, de Almeida Ribeiro Oliveira G, Lião LM, Franco Dos Santos G, Vaz BG, Sabino JR, Alcantara Dos Santos FC, Costa EA, Tarozzi A, Menegatti R, Ghedini PC., 2024. Chrysin bonded to β-d-glucose tetraacetate enhances its protective effects against the neurotoxicity induced by aluminum in Swiss mice. J Pharm Pharmacol. rgae011. https://doi.org/ 10.1093/jpp/rgae011

[16] Ontario ML, Siracusa R, Modafferi S, Scuto M, Sciuto S, Greco V, Bertuccio MP, Trovato Salinaro A, Crea R, Calabrese EJ, Di Paola R, Calabrese V., 2022. Potential prevention and treatment of neurodegenerative disorders by olive polyphenols and hidrox. Mech Ageing Dev. 203:111637. https://doi.org/ 10.1016/j.mad.2022.111637

[17] Catanesi M, Caioni G, Castelli V, Benedetti E, d'Angelo M, Cimini A., 2021. Benefits under the Sea: The Role of Marine Compounds in Neurodegenerative Disorders. Mar Drugs. 19(1):24. https://doi.org/10.3390/md19010024

[18] Guimarães PL, Tavares DQ, Carrião GS, Oliveira MEH, Oliveira CR., 2023. Potential of marine compounds in the treatment of neurodegenerative diseases: a review. Braz J Biol. 83:e266795. https://doi.org/10.1590/1519-6984.266795

[19] Popovic M, Stanojevic Z, Tosic J, Isakovic A, Paunovic V, Petricevic S, Martinovic T, Ciric D, Kravic-Stevovic T, Soskic V, Kostic-Rajacic S, Shakib K, Bumbasirevic V, Trajkovic V., 2015. Neuroprotective arylpiperazine dopaminergic/serotonergic ligands suppress experimental autoimmune encephalomyelitis in rats. J Neurochem. 135(1):125-38. https://doi.org/10.1111/jnc.13198

[20] Andonova L, Valkova I, Zheleva-Dimitrova D, Georgieva M, Momekov G, Zlatkov A., 2019. Synthesis of New N1Arylpiperazine Substituted Xanthine Derivatives and Evaluation of their Antioxidant and Cytotoxic Effects. Anticancer Agents Med Chem. 19(4):528-537. https://doi.org/10.2174/1871520619666190121155651

[21] Glomb T, Wiatrak B, Gębczak K, Gębarowski T, Bodetko D, Czyżnikowska Ż, Świątek P., 2020. New 1,3,4-Oxadiazole Derivatives of Pyridothiazine-1,1-Dioxide with Anti-Inflammatory Activity. Int J Mol Sci. 21(23):9122. doi: 10.3390/ijms21239122

[22] Pietrzycka A, Stepniewski M, Waszkielewicz AM, Marona H., 2006. Preliminary evaluation of antioxidant activity of some 1-(phenoxyethyl)-piperazine derivatives. Acta Pol Pharm. 63(1):19-24. PMID: 17515325

[23] Brito, A.F., Braga, P.C.C.S., Moreira, L.K.S. et al., 2018. A new piperazine derivative: 1-(4-(3,5-di-tert-butyl-4-hydroxybenzyl) piperazin-1-yl)-2-methoxyethan-1-one with antioxidant and central activity. Naunyn-Schmiedeberg's Arch Pharmacol 391, 255–269 . https://doi.org/10.1007/s00210-017-1451-7

[24] Begum S., Rashida Anjum M., Poojitha Harisree G., Sivalakshmi N., Priyanka P., Bharathi K. ,2020. Antioxidant Activity of Piperazine Compounds: A Brief Review. Asian Journal of Chemistry, 32(9), 2105-2118. https://doi.org/10.14233/ajchem.2020.22832

[25] Cumbo E, Cumbo S, Torregrossa S, Migliore D., 2019. Treatment Effects of Vortioxetine on Cognitive Functions in Mild Alzheimer's Disease Patients with Depressive Symptoms: A 12 Month, Open-Label, Observational Study. J Prev Alzheimers Dis. 6(3):192-197. https://doi.org/10.14283/jpad.2019.24

[26] La AL, Walsh CM, Neylan TC, Vossel KA, Yaffe K, Krystal AD, Miller BL, Karageorgiou E., 2019. Long-Term Trazodone Use and Cognition: A Potential Therapeutic Role for Slow-Wave Sleep Enhancers. J Alzheimers Dis. 67(3):911-921. https://doi.org/10.3233/JAD-181145

[27] Dourish, C., and Colin T., 1983. Piribedil: behavioral, neurochemical and clinical profile of a dopamine agonist.: Behavioral, neurochemical and clinical profile of a dopamine agonist. Progress in Neuro-psychopharmacology and Biological Psychiatry. 7, 3-27. https://doi.org/ 10.1016/0278-5846(83)90085-4

[28] Jenner, P., 1992. Parkinson's disease: pathological mechanisms and actions of piribedil. Journal of Neurology. 239, 2–8. https://doi.org/ 10.1007/BF00819559

[29] Peihua, L., and Jianqin, W., 2018. Clinical effects of piribedil in adjuvant treatment of Parkinson's disease: A meta-analysis. Open Medicine. 1, 270-277. https://doi.org/10.1515/med-2018-0041

[30] Smith, L., Jackson, M., Bonhomme C., et al., 2000. Transdermal administration of piribedil reverses MPTP-induced motor deficits in the common marmoset. Clinical Neuropharmacology. 23, 133-142. https://doi.org/ 10.1097/00002826-200005000-00002

[31] Wang, W., Liu, L., Chen, C., Jiang, P., Zhang, T., 2018. Protective effects of dopamine D2/D3 receptor agonist piribedil on learning and memory of rats exposed to global cerebral ischemia–reperfusion. Neuroscience Letters. 684, 181-186. https://doi.org/10.1016/j.neulet.2018.08.011

[32] Moreira LKDS, Turones LC, Campos HM, Nazareth AM, Thomaz DV, Gil ES, Ghedini PC, Rocha FFD, Menegatti R, Fajemiroye JO, Costa EA., 2023. LQFM212, a piperazine derivative, exhibits potential antioxidant effect as well as ameliorates LPS-induced behavioral, inflammatory and oxidative changes. Life Sci. 312:121199. https://doi.org/10.1016/j.lfs.2022.121199

[33] Mastromarino M, Niso M, Abate C, Proschak E, Dubiel M, Stark H, Castro M, Lacivita E, Leopoldo M., 2022. Design and Synthesis of Arylpiperazine Serotonergic/Dopaminergic Ligands with Neuroprotective Properties. Molecules. 27(4):1297. https://doi.org/10.3390/molecules27041297

[34] Guardigni M, Pruccoli L, Santini A, Simone A, Bersani M, Spyrakis F, Frabetti F, Uliassi E, Andrisano V, Pagliarani B, Fernández-Gómez P, Palomo V, Bolognesi ML, Tarozzi A, Milelli A., 2023. PROTAC-Induced Glycogen Synthase Kinase 3β Degradation as a Potential Therapeutic Strategy for Alzheimer's Disease. ACS Chem Neurosci. 14(11):1963-1970. https://doi.org/10.1021/acschemneuro.3c00096

[35] Ortiz, C.J.C., Damasio, C.M., Pruccoli, L., Nadur, N.F., de Azevedo, L.L., Guedes, I.A., Dardenne, L.E., Kümmerle, A.E., Tarozzi, A., Viegas, C.J., 2020. Cinnamoyl-n-acylhydrazone-donepezil hybrids: synthesis and evaluation of novel multifunctional ligands against neurodegenerative diseases. Neurochemical Research. 45, 3003–3020. https://doi.org/10.1007/s11064-020-03148-2

[36] Pruccoli L, Morroni F, Sita G, Hrelia P, Tarozzi A., 2020. Esculetin as a Bifunctional Antioxidant Prevents and Counteracts the Oxidative Stress and Neuronal Death Induced by Amyloid Protein in SH-SY5Y Cells. Antioxidants (Basel). 9(6):551. https://doi.org/10.3390/antiox9060551

[37] Di Martino RMC, Pruccoli L, Bisi A, Gobbi S, Rampa A, Martinez A, Pérez C, Martinez-Gonzalez L, Paglione M, Di Schiavi E, Seghetti F, Tarozzi A, Belluti F., 2020. Novel Curcumin-Diethyl Fumarate Hybrid as a Dualistic GSK-3β Inhibitor/Nrf2 Inducer for the

Treatment of Parkinson's Disease. ACS Chem Neurosci. 11(17):2728-2740. https://doi.org/10.1021/acschemneuro.0c00363

[38] Abdelfattah MS, Badr SEA, Lotfy SA, Attia GH, Aref AM, Abdel Moneim AE, Kassab RB., 2020. Rutin and Selenium Co-administration Reverse 3-Nitropropionic Acid-Induced Neurochemical and Molecular Impairments in a Mouse Model of Huntington's Disease. Neurotox Res. 37(1):77-92. https://doi.org/10.1007/s12640-019-00086-y

[39] Antiorio, AT., Alemán-Laporte J., Zanatto DA., Pereira MAA., Gomes MS, Wadt D, Yamamoto PK, Bernardi MM, Mori CM., 2022. Mouse Behavior in the Open-field Test after Meloxicam Administration. J Am Assoc Lab Anim Sci. 61(3):270-274. https://doi.org/10.30802/AALAS-JAALAS-21-000046

[40] Collenberg, V., Schmitt, D., Rülicke, T., Sendtner, M., Blum, R., Buchner, E., 2019. An essential role of the mouse synapse-associated protein Syap1 in circuits for spontaneous motor activity and rotarod balance. Biology Open. 8, 1-20. https://doi.org/10.1242/bio.042366

[41] Campos HM, da Costa M, da Silva Moreira LK, da Silva Neri HF, Branco da Silva CR, Pruccoli L, Dos Santos FCA, Costa EA, Tarozzi A, Ghedini PC., 2022. Protective effects of chrysin against the neurotoxicity induced by aluminium: In vitro and in vivo studies. Toxicology. 465:153033. https://doi.org/10.1016/j.tox.2021.153033

[42] Brondani M, Roginski AC, Ribeiro RT, de Medeiros MP, Hoffmann CIH, Wajner M, Leipnitz G, Seminotti B., 2023. Mitochondrial dysfunction, oxidative stress, ER stress and mitochondria-ER crosstalk alterations in a chemical rat model of Huntington's disease: Potential benefits of bezafibrate. Toxicol Lett. 381:48-59 . https://doi.org/10.1016/j.toxlet.2023.04.011

[43] Menegatti R, Cunha AC, Ferreira VF, Perreira EF, El-Nabawi A, Eldefrawi AT, Albuquerque EX, Neves G, Rates SM, Fraga CA, Barreiro EJ., 2003. Design, synthesis and pharmacological profile of novel dopamine D2 receptor ligands. Bioorg Med Chem. 11(22):4807-13. . https://doi.org/10.1016/s0968-0896(03)00487-5

[44] Kumar, P., and Kumar, A., 2009. Protective effect of rivastigmine against 3-nitropropionic acid-induced Huntington's disease like symptoms: Possible behavioral, biochemical and cellular alterations. European Journal of Pharmacology. 615, 91-101. https://doi.org/10.1016/j.ejphar.2009.04.058

[45] Liu, P., Li, Y., Liu, D., Ji, X., Chi, T., Li, L., Zou, L., 2018. Tolfenamic Acid Attenuates 3-Nitropropionic Acid-Induced Biochemical Alteration in Mice. Neurochemical Research. 43, 1938-1946. https://doi.org/10.1007/s11064-018-2615-7

[46] Atessahin, A., Ceribasi, O., Yilmaz, S., 2007. Lycopene, a carotenoid, attenuates cyclosporine-induced renal dysfunction and oxidative stress in rats. Basic Clinical Pharmacology and Toxicology. 100, 372–376. https://doi.org/10.1111/j.1742-7843.2007.00060.x

[47] Kaur, N., Jamwal, S., Deshmukh, R., Gauttam, V., Kumar, P., 2015. Beneficial effect of rice bran extract against 3-nitropropionic acid induced experimental Huntington's disease in rats. Toxicology Reports. 2, 1222-1232. https://doi.org/10.1016/j.toxrep.2015.08.004

[48] Malik, J., Karan, M., Dogra, R., 2017. Ameliorating effect of *Celastrus paniculatus* standardized extract and its fractions on 3-nitropropionic acid induced neuronal damage in rats: Possible antioxidant mechanism. Pharmaceutical Biology. 55, 980-990. https://doi.org/10.1080/13880209.2017.1285945

[49] Danduga RCSR, Dondapati SR, Kola PK, Grace L, Tadigiri RVB, Kanakaraju VK., 2018. Neuroprotective activity of tetramethylpyrazine against 3-nitropropionic acid induced Huntington's disease-like symptoms in rats. Biomed Pharmacother. 105:1254-1268. https://doi.org/ 10.1016/j.biopha.2018.06.079

[50] Duckworth, E.A., Koutouzis, T.K., Borlongan, C.V. et al., 1999. Rats receiving systemic 3-nitropropionic acid demonstrate impairment of memory in Morris water maze. Psychobiology 27, 561–566. https://doi.org/10.3758/BF03332154

[51] Akashiba H, Ikegaya Y, Nishiyama N, Matsuki N., 2008. Differential involvement of cell cycle reactivation between striatal and cortical neurons in cell death induced by 3-nitropropionic acid. J Biol Chem. 283(10):6594-606. https://doi.org/10.1074/jbc.M707730200

[52] Kumar, P., Kalonia, H., Kumar, A., 2009. Lycopene modulates nitric oxide pathways against 3-nitropropionic acid-induced neurotoxicity. Life Sciences. 85, 711-718. https://doi.org/10.1016/j.lfs.2009.10.001

[53] Ludolph AC, He F, Spencer PS, Hammerstad J, Sabri M., 1991. 3-Nitropropionic acid-exogenous animal neurotoxin and possible human striatal toxin. Can J Neurol Sci. 18(4):492-8. https://doi.org/10.1017/s0317167100032212

[54] Binienda Z, Simmons C, Hussain S, Slikker W Jr, Ali SF., 1998. Effect of acute exposure to 3-nitropropionic acid on activities of endogenous antioxidants in the rat brain. Neurosci Lett. 251(3):173-6. https://doi.org/10.1016/s0304-3940(98)00539-4

[55] Mehan S, Monga V, Rani M, Dudi R, Ghimire K., 2018. Neuroprotective effect of solanesol against 3-nitropropionic acid-induced Huntington's disease-like behavioral, biochemical, and cellular alterations: Restoration of coenzyme-Q10-mediated mitochondrial dysfunction. Indian J Pharmacol. 50(6):309-319. https://doi.org/10.4103/ijp.IJP_11_18

[56] Sadashiva CT, Narendra Sharath Chandra JN, Ponnappa KC, Veerabasappa Gowda T, Rangappa KS., 2006. Synthesis and efficacy of 1-[bis(4-fluorophenyl)-methyl]piperazine derivatives for acetylcholinesterase inhibition, as a stimulant of central cholinergic neurotransmission in Alzheimer's disease. Bioorg Med Chem Lett. 16(15):3932-6. https://doi.org/10.1016/j.bmcl.2006.05.030

[57] Aranha CMSQ, Reiner-Link D, Leitzbach LR, Lopes FB, Stark H, Fernandes JPS., 2023. Multitargeting approaches to cognitive impairment: Synthesis of aryl-alkylpiperazines and assessment at cholinesterases, histamine H3 and dopamine D3 receptors. Bioorg Med Chem. 78:117132. https://doi.org/10.1016/j.bmc.2022

[58] Kaur, M., Prakash, A., Kalia, A., 2016. Neuroprotective potential of antioxidant potent fractions from Convolvulus pluricaulis Chois. in 3-nitropropionic acid challenged rats. Nutritional Neuroscience. 8305, 1-9. https://doi.org/10.1080/1028415x.2015.1107277

[59] Suganya, S., Sumathi, T., 2017. Effect of rutin against a mitochondrial toxin, 3-nitropropionicacid induced biochemical, behavioral and histological alterations-a pilot study on Huntington's disease model in rats. Metabolic Brain Disease. 32, 471-481. https://doi.org/10.1007/s11011-016-9929-4

[60] Malik, J., Kaur, S., Karan, M., Choudhary, S., 2020. Neuroprotective effect of standardized extracts of three Lactuca sativa Linn. varieties against 3-NP induced Huntington's disease like symptoms in rats. Nutritional Neuroscience. 1, 1–15. https://doi.org/10.1080/1028415X.2020.1841500

[61] Wullner, U., Young, A., Penney, J., Beal, M., 1994. 3-Nitropropionic acid toxicity in the striatum. Journal of Neurochemistry. 63(5), 1772–1781. https://doi.org/10.1046/j.1471-4159.1994.63051772.x

[62] Browne, S., Bowling, A., MacGarvey, U., et al., 1997. Oxidative damage and metabolic dysfunction in Huntington's disease: selective vulnerability of the basal ganglia. Annals of Neurology. 41, 646–653. https://doi.org/10.1002/ana.410410514

[63] Jodeiri Farshbaf M, Kiani-Esfahani A., 2018. Succinate dehydrogenase: Prospect for neurodegenerative diseases. Mitochondrion. 42:77-83. https://doi.org/10.1016/j.mito.2017.12.002

[64] Bortolatto, C., Jesse, C., Wilhelm, E., Chagas, P., Nogueira, C., 2013. Organoselenium bis selenide attenuates 3-nitropropionic acid-induced neurotoxicity in rats. Neurotoxicity Research. 23, 214-224. https://doi.org/10.1007/s12640-012-9336-5

[65] Kumar B, Kumar N, Thakur A, Kumar V, Kumar R, Kumar V., 2022. A Review on the Arylpiperazine Derivatives as Potential Therapeutics for the Treatment of Various Neurological

Disorders. Curr Drug Targets. 23(7):729-751. https://doi.org/10.2174/1389450123666220117104038

[66] Bajad NG, Singh RB, T A G, Gutti G, Kumar A, Krishnamurthy S, Singh SK., 2024. Development of multi-targetable chalcone derivatives bearing N-aryl piperazine moiety for the treatment of Alzheimer's disease. Bioorg Chem. 43:107082. https://doi.org/10.1016/j.bioorg.2023.107082

[67] Hussain T, Tan B, Yin Y, Blachier F, Tossou MC, Rahu N., 2016. Oxidative Stress and Inflammation: What Polyphenols Can Do for Us? Oxid Med Cell Longev. 7432797. https://doi.org/10.1155/2016/7432797